

- trometry and Allied Topics, San Antonio, May 1984, pp. 546-547.
29. T. Francl, M. G. Sherman, R. L. Hunter, M. J. Locke, W. D. Bowers, R. T. McIver, Jr., *Int. J. Mass Spectrom. Ion Phys.* **54**, 189 (1983).
 30. J. L. Beauchamp and J. T. Armstrong, *Rev. Sci. Instrum.* **40**, 123 (1969).
 31. E. B. Ledford, Jr., S. Ghaderi, R. L. White, R. B. Spencer, P. S. Kulkarni, C. L. Wilkins, M. L. Gross, *Anal. Chem.* **52**, 463 (1980).
 32. M. Alleman, Hp. Kellerhals, K.-P. Wanczek, *Chem. Phys. Lett.* **84**, 547 (1981).
 33. E. B. Ledford, Jr., D. L. Rempel, M. L. Gross, *Anal. Chem.*, in press.
 34. R. L. White, E. C. Onyiriuka, C. L. Wilkins, *ibid.* **55**, 339 (1983).
 35. E. B. Ledford, Jr., R. L. White, S. Ghaderi, C. L. Wilkins, M. L. Gross, *ibid.* **52**, 2450 (1980).
 36. R. L. White and C. L. Wilkins, *ibid.* **54**, 2443 (1982).
 37. C. L. Wilkins, G. N. Giss, R. L. White, G. M. Brissey, E. M. Onyiriuka, *ibid.*, p. 2261.
 38. T. M. Sack and M. L. Gross, *ibid.* **55**, 2421 (1983).
 39. R. J. Cotter, *ibid.* **56**, 485A (1984).
 40. R. B. Bernstein, *J. Phys. Chem.* **86**, 1178 (1982).
 41. M. P. Irion, W. D. Bowers, R. L. Hunter, F. S. Rowland, R. T. McIver, Jr., *Chem. Phys. Lett.* **93**, 375 (1982).
 42. T. J. Carlin and B. S. Freiser, *Anal. Chem.* **55**, 955 (1983).
 43. G. Rhodes, R. B. Opsal, J. T. Meek, J. P. Reilly, *ibid.*, p. 280.
 44. T. M. Sack, D. A. McCrery, M. L. Gross, paper presented at the 32nd Annual Conference on Mass Spectrometry and Allied Topics, San Antonio, May 1984, pp. 591-592.
 45. M. A. Posthumus, P. G. Kistemaker, H. L. C. Meuzelaar, M. C. Ten Noever deBrauw, *Anal. Chem.* **50**, 985 (1978).
 46. R. C. Burnier *et al.*, *J. Am. Chem. Soc.* **101**, 7127 (1979).
 47. D. A. McCrery, E. B. Ledford, Jr., M. L. Gross, *Anal. Chem.* **54**, 1437 (1982).
 48. R. J. Cotter and J.-C. Tabet, *Int. J. Mass Spectrom. Ion Phys.* **53**, 151 (1983).
 49. R. L. Hunter and R. T. McIver, Jr., *Anal. Chem.* **51**, 699 (1979).
 50. S. Ghaderi, P. S. Kulkarni, E. B. Ledford, Jr., C. L. Wilkins, M. L. Gross, *ibid.* **53**, 428 (1981).
 51. D. F. Hunt, C. N. McEwen, R. A. Upham, *ibid.* **44**, 1291 (1972).
 52. T. M. Sack and M. L. Gross, paper presented at the 31st Annual Conference on Mass Spectrometry and Allied Topics, Boston, May 1983, pp. 396-397.
 53. R. C. Dunbar, in *Gas-Phase Ion Chemistry*, M. T. Bowers, Ed. (Academic Press, New York, 1979), pp. 182-220.
 54. R. C. Dunbar, in *Ionic Processes in the Gas-Phase*, M. A. Almoester Ferreira, Ed. (Reidel, Dordrecht, 1984), pp. 179-204.
 55. W. D. Bowers, S. S. Delbert, R. T. McIver, Jr., paper presented at the 32nd Annual Conference on Mass Spectrometry and Allied Topics, San Antonio, May 1984, pp. 337-338.
 56. R. B. Cody and B. S. Freiser, *Int. J. Mass Spectrom. Ion Phys.* **41**, 199 (1982).
 57. R. T. McIver, Jr., and W. D. Bowers, in *Tandem Mass Spectrometry*, F. W. McLafferty, Ed. (Wiley, New York, 1983), pp. 287-302.
 58. F. W. McLafferty, *Science* **214**, 280 (1981).
 59. D. L. Bricker, T. A. Adams, Jr., D. H. Russell, *Anal. Chem.* **55**, 2417 (1983).
 60. R. B. Cody and B. S. Freiser, *ibid.* **54**, 1431 (1982).
 61. R. L. White and C. L. Wilkins, *ibid.*, p. 2211.
 62. T. J. Carlin and B. S. Freiser, *ibid.* **55**, 571 (1983).
 63. J. C. Kleingeld, thesis, University of Amsterdam (1984).
 64. M. T. Bowers, Ed., *Gas-Phase Ion Chemistry* (Academic Press, New York, 1979), vols. 1 and 2.
 65. H. Hartmann and K.-P. Wanczek, Eds., *Lecture Notes in Chemistry* (Springer-Verlag, Berlin, 1982), vol. 31.
 66. M. A. Almoester Ferreira, *Ionic Processes in the Gas-Phase* (Reidel, Dordrecht, 1984).
 67. J. C. Kleingeld and N. M. M. Nibbering, *Org. Mass Spectrom.* **17**, 136 (1982).
 68. T. C. Jackson, D. B. Jacobson, B. S. Freiser, *J. Am. Chem. Soc.* **106**, 1252 (1984).
 69. C. Dass, T. M. Sack, M. L. Gross, *ibid.*, in press.
 70. D. L. Smith and J. H. Futrell, *Int. J. Mass Spectrom. Ion Phys.* **14**, 171 (1974).
 71. P. R. Kemper and M. T. Bowers, *ibid.* **52**, 1 (1983).
 72. R. T. McIver, Jr., R. L. Hunter, W. D. Bowers, paper presented at the 32nd Annual Conference on Mass Spectrometry and Allied Topics, San Antonio, May 1984.
 73. R. T. McIver, Jr., and D. Hunt, private communication.
 74. A. G. Marshall, T.-C. Wang, T. L. Ricca, paper presented at the 32nd Annual Conference on Mass Spectrometry and Allied topics, San Antonio, May 1984, pp. 600-601.
 75. Some of the research reported here has been supported by funds from the National Science Foundation (grant CHE 8018245) and the National Institutes of Health (grant 2-8423576). 423576.

Pyrolysis Mass Spectrometry of Complex Organic Materials

Henk L. C. Meuzelaar, Willem Windig, Alice M. Harper
Stanley M. Huff, William H. McClennen, Joseph M. Richards

High sensitivity, specificity, and speed are widely recognized characteristics of mass spectrometry (MS) which have earned the technique its reputation as one of the most powerful analytical tools for organic materials available today. With the total number of library spectra approaching 100,000 and with novel desorption ionization methods such as fast atom bombardment advancing into the 5,000- to 15,000-dalton range (1), it is tempting to credit MS with nearly universal applicability as well. Unfortunately, in reality most organic materials on this planet, whether natural or man-made, consist of molecular assemblies of a complexity and size far beyond the capabilities of direct MS techniques.

As we intend to demonstrate in this article, however, the combined use of advanced pyrolysis techniques, mass

spectrometry, and computerized multivariate analysis methods (Py-MS) offers a viable approach to the analysis of extremely complex organic materials. Moreover, Py-MS techniques require minimal sample preparation and can be readily automated (2, 3). On the negative side, however, these techniques have not yet attained a satisfactory level of interlaboratory reproducibility and require dedicated equipment and expert personnel.

During the past two years, several comprehensive overviews of the development of Py-MS techniques since Zeman's pioneering work in 1952 (4) were published by Irwin (2), by Meuzelaar *et al.* (3), and by Schulten and Latimer (5). These monographs provide in-depth discussions of the different Py-MS techniques and their applications in the areas

of synthetic polymer chemistry, natural product chemistry, biochemistry, pharmacology, microbiology, medicine, fuels technology, organic geochemistry, soil science, and forensic science.

As schematically depicted in Fig. 1, the three basic pyrolysis techniques (filament pyrolysis, direct probe pyrolysis, and laser pyrolysis) may be combined with any of a number of different mass separation techniques and chemometric procedures, which explains the multitude of experimental approaches encountered in the literature. Nevertheless, filament pyrolysis techniques appear to be the method of choice in most current reports and Curie-point Py-MS (perhaps the most widely used form of filament Py-MS today) has achieved a limited degree of standardization and interlaboratory reproducibility (3) due to the availability of dedicated Curie-point Py-MS systems from at least two manufacturers (6).

The present article will not attempt to provide a comprehensive overview of the many different Py-MS techniques and procedures, such as can be found in the above referenced monographs. In-

Henk L. C. Meuzelaar is a research professor and director of the Biomaterials Profiling Center, University of Utah, Salt Lake City 84108. Willem Windig, William H. McClennen, and Joseph M. Richards are on the staff of the Biomaterials Profiling Center, as research associate, analytical chemist, and research assistant, respectively. Stanley M. Huff is a resident in the Department of Pathology at the University of Utah School of Medicine, and Alice M. Harper is an assistant professor of chemistry at the University of Texas, El Paso 79968.

stead, the experiments discussed in the next paragraphs were selected to highlight some of the most recent capabilities of Py-MS in general and of Curie-point Py-MS in particular.

Methods and Procedures

Sample preparation. Most filament pyrolysis MS techniques require the sample to be coated on a metal wire or ribbon from a relatively dilute solution or suspension. Occasionally the sample can be applied directly to the filament in the form of a paste [for instance, bacterial colonies sampled directly from agar plates (3)], a wet powder, or a thin fiber (which can be wound around the filament).

Typical sample preparation procedures for insoluble materials in Curie-point Py-MS involve the production of a fine, homogeneous suspension in methanol, phosphate buffer, or other suitable solvent, using 1 to 2 mg of sample per milliliter of solvent. One or two 5- μ l drops of this suspension are then applied to the ferromagnetic wires used in Curie-point pyrolysis and air-dried under slow, continuous rotation, thus producing a 5- to 20- μ g sample coating on the wire.

As discussed by several authors (3, 7), the choice of the solvent can have a marked effect on the pyrolysis patterns, especially in the case of highly polar materials and/or in the presence of alkali cations. Moreover, the filament cleaning procedure (such as solvent cleaning, reductive hydrogenation, vacuum heating, or "firing" in a flame) has a significant effect on the pyrolysis patterns as well (3, 7, 8).

Pyrolysis mass spectrometry. The Curie-point Py-MS technique illustrated in Fig. 2 was used in all experiments described in the Results and Discussion section. The sample is pyrolyzed directly in front of the ion source by means of a high-frequency field (≈ 1 MHz), which causes inductive heating of the ferromagnetic wire on which the sample has been coated. Depending on the strength of the field, the wire may heat up to the Curie-point temperature of the ferromagnetic alloy in a time as short as 100 msec or as long as 5 seconds. Under appropriately selected frequency and field strength conditions, as well as dimensions and alloys of the wires, the temperature of the latter will automatically stabilize within a few degrees Celsius of the Curie-point temperature (358°C for Ni, 770°C for Fe, 1128°C for Co; intermediate values for various ferromagnetic alloys).

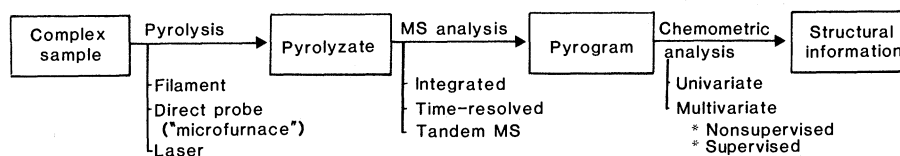
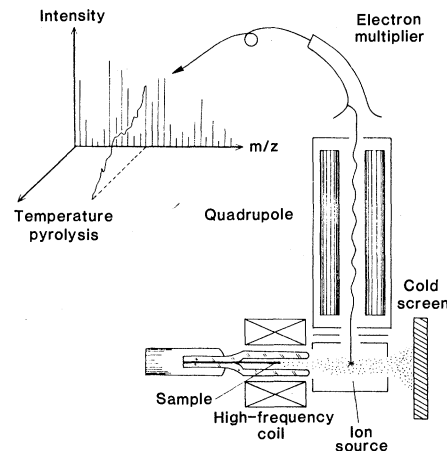


Fig. 1. Basic approach options to computerized pyrolysis mass spectrometry.

Fig. 2. Schematic diagram of a basic Curie-point Py-MS system. Typical operating conditions: temperature rise time, 5 seconds; total heating time, 10 seconds; electron energy, 12 to 15 eV; scanning speed, 1000 amu/sec; total scanning time, 20 seconds. Note optional availability of time-resolved (and thus temperature-resolved) signals.



The Curie-point pyrolysis method was developed for gas chromatography in 1964 by Simon and co-workers at the ETH in Zurich (9) and adapted for Py-MS of polymeric materials by Meuzelaar and Kistemaker in 1972 (10). Initially, a gold-coated, preheated expansion chamber was positioned between the reaction chamber and the ion source (3, 10). In later experiments the expansion chamber was omitted in order to enable time-

and prevent buildup of deposits elsewhere in the system (3). The ion source is usually operated at low electron energies (11 to 15 eV) in order to reduce ion fragmentation tendencies and to suppress background contributions from permanent gases (13). During the 10 to 20 seconds or so that a measurable pressure rise occurs in the ion source due to the pyrolysis event, the quadrupole mass spectrometer is repetitively scanned

Summary. Pyrolysis mass spectrometry in combination with computerized multivariate statistical analysis enables qualitative and quantitative analysis of nonvolatile organic materials containing molecular assemblies of a complexity and size far beyond the capabilities of direct mass spectrometry. The state of the art in pyrolysis mass spectrometry techniques is illustrated through specific applications, including structural determination and quality control of synthetic polymers, quantitative analysis of polymer mixtures, classification and structural characterization of fossil organic matter, and nonsupervised numerical extraction of component patterns from complex biological samples.

resolved recording of pyrolysis events (11), as shown in Fig. 2. However, most of the six or seven different laboratories which currently have more or less compatible Curie-point Py-MS instruments (12) still use the expansion chamber for all routine work.

As shown in Fig. 2, the pyrolysis products are allowed to diffuse into an open, cross-beam type electron impact ionizer surrounded by a large, liquid nitrogen-cooled trap. This cold trap serves as an efficient cryopump for all organic pyrolysis products not ionized during their first pass through the ionization chamber. This helps reduce background signals

over the desired mass range at high speed (for instance, 1000 atomic mass units per second) and the resulting spectra either summed (integrated mode) or sequentially recorded (time-resolved mode). Because of the low signal intensities and high scan speed requirements, fast (for instance, 100 MHz) ion counting methods are preferred over analog signal recording techniques.

Besides the basic Curie-point Py-MS technique shown in Fig. 2, several more specialized Py-MS methods have been developed which can provide highly valuable additional information on the chemical identity and origin of the pyrol-

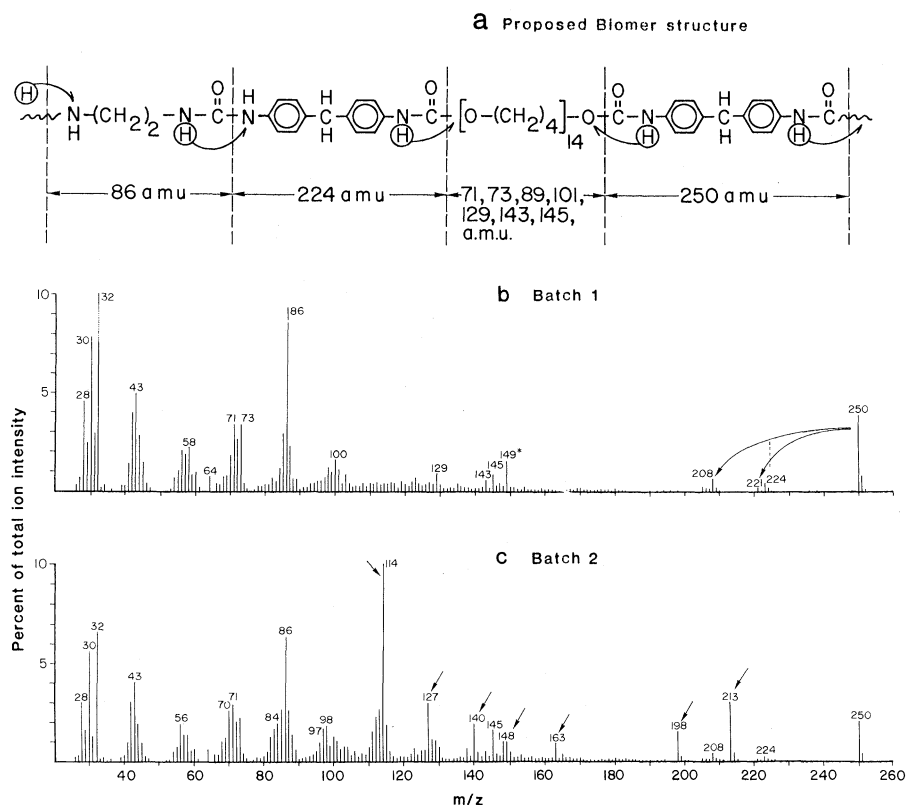


Fig. 3. The proposed structure of the poly(ether urethane urea) Biomer in (a) corresponds to the low-voltage Curie-point pyrolysis mass spectrum of batch 1 in (b). The spectrum of batch 2 in (c) reveals an additional peak series (see arrows) believed to represent a quaternary (alkyl)ammonium compound. Experimental conditions: 5- μ g samples coated from a solution in dimethylacetamide; 610°C (Curie-point temperature) wires; temperature rise time, 5 seconds; electron energy, 12 eV (set value).

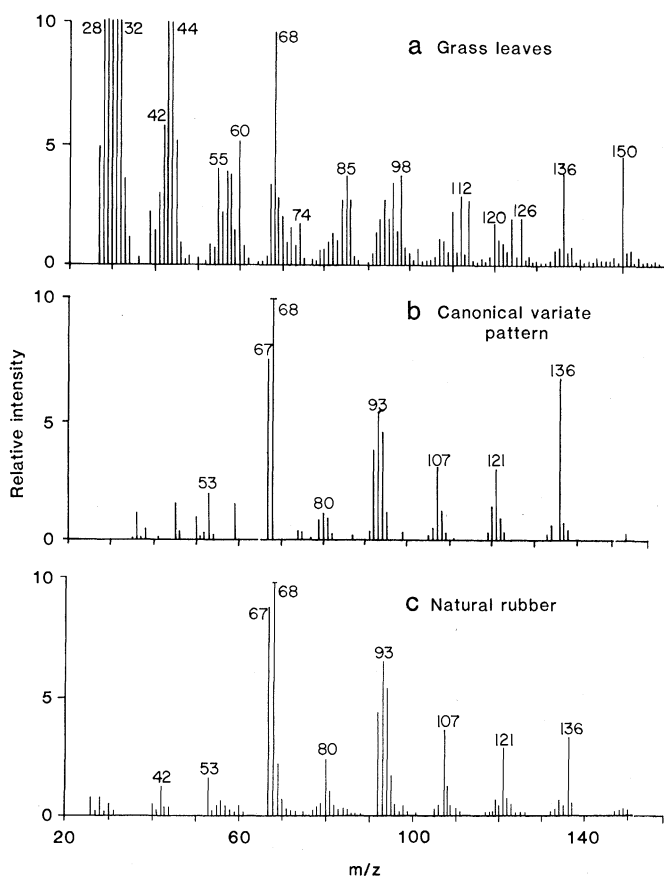


Fig. 4. (a) Low-voltage Curie-point pyrolysis mass spectrum of grass leaves, representing the average intensity values of a set of eight senescent leaf samples analyzed in triplicate. (b) Component pattern extracted by canonical variate analysis and showing a strong positive correlation (coefficient = 0.97) with susceptibility to insect attack. (c) Spectrum of natural rubber obtained from (3). Experimental conditions: 20- μ g leaf samples were coated from a methanol suspension; for further details see legend to Fig. 3.

ysis products. Examples of such specialized methods are: CO₂ laser pyrolysis MS (14), pyrolysis high-resolution MS (Py-HRMS) (15), pyrolysis tandem MS (Py-MS-MS) (11), pyrolysis time-resolved MS (Py-TRMS) (11), and Py-MS in combination with various other "soft ionization" methods, such as field ionization (16), field desorption (17), or chemical ionization (18). In our laboratory, Py-TRMS and Py-MS-MS are frequently called upon to provide additional information (see also Fig. 1).

Computerized data analysis. As shown in Fig. 1, computerized data analysis is an integral part of the analytical pyrolysis procedure. In fact, due to the rapid developments in this area, which have resulted in a multiplicity of available techniques and options, computerized data analysis is fast becoming the most rewarding (and most time-consuming) step in the procedure. A typical data analysis sequence proceeds from routine mass calibration and peak calculation procedures through more specialized normalization programs to the multivariate analysis stage.

As discussed elsewhere (2, 3, 19), proper normalization of the total spectrum intensity is of crucial importance. The basic principle behind the normalization approach used in most of our studies (19) is to exempt all mass peaks with major variance contributions from the normalization procedure. In other words, the stable, "common" part of the pyrolysis patterns in the data set is used as an internal standard in order to avoid propagation of measurement errors (due to peaks with high "within-category" variance) or creation of pseudocorrelations (due to peaks with high "between-category" variance). This normalization procedure is carried out in an iterative manner, using the operator-interactive program NORMA (20). The normalized data can then be analyzed by multivariate statistical analysis routines such as are available in the ARTHUR (21) or SPSS (22) program package.

A routine, nonsupervised multivariate analysis run consists of factor analysis followed by discriminant analysis, using the first 10 or 12 most significant factors and regarding each set of replicate analyses of a sample as a separate category (23). The most striking result of these multivariate analysis procedures is the sharp reduction in apparent dimensionality of the data. From an initial collection of several hundred mass peaks the data are reduced to only a few factors or discriminant functions, each of which is by definition a linear combination of the

original mass peak intensities. Moreover, by plotting these linear combinations in the form of "spectra" (23) the operator obtains a wealth of information about the chemical tendencies or components underlying the factors. Often this requires "graphical rotation" of the factors (24) in order to optimize the chemical component patterns.

Recently, a nonsupervised factor rotation method was developed by Windig and Meuzelaar (25). This technique, the so-called variance diagram method, holds considerable promise for fully automated interpretation of complex pyrolysis mass spectra in the near future. Other multivariate analysis methods which are frequently used in Py-MS applications include canonical variate analysis (26), nonlinear mapping (27), SIMCA (28), hierarchical clustering dendrograms (29), K-nearest neighbor tables (30), and distance matrices (27). In particular, the use of canonical variate analysis and related methods for correlating data matrices obtained by different spectrometric, chromatographic, or other techniques promises to revolutionize the integration of measurement results in tomorrow's analytical laboratory.

Results and Discussion

In order to demonstrate the capabilities of modern Py-MS techniques a number of different applications will be discussed, starting with relatively simple materials such as synthetic polymers and moving toward extremely complex biochemical systems such as whole microorganisms.

Structural analysis of synthetic polymers. The spectrum of Biomer, a commercial poly(ether urethane urea) (PEU) used in the construction of artificial hearts and other cardiovascular implants, demonstrates (Fig. 3b) that Py-MS analysis can provide detailed structural information on relatively pure polymeric materials. All three major building blocks, namely (i) the polyol (polytetramethyleneglycol-characteristic fragment ion peaks at mass-to-charge ratio m/z 71, 73, 143, and 145); (ii) the isocyanate (diisocyanato diphenylmethane-molecular ion at m/z 250, fragment ions at m/z 221 and 208); and (iii) the chain extender (ethylenediamine-carbonylated molecular ion at m/z 86, fragment ion at m/z 30, and isocyanate-derived amine at m/z 224), are clearly represented. The presence of characteristic chain extender signals is particularly exciting since detection of these moieties by other spectro-

metric techniques, infrared or nuclear magnetic resonance (NMR) spectroscopy, is notoriously difficult (29).

The structural assignments in Fig. 3a were further supported by Py-HRMS, Py-TRMS, and Py-MS-MS experiments. Final confirmation of the proposed structure was obtained by synthesizing a model polymer with a Py-MS pattern closely resembling that of the commercial polyurethane pattern in Fig. 3b (30).

Quality control of polymer batches. In contrast, the spectrum shown in Fig. 3c, which represents a different batch of the same commercially available PEU, reveals the presence of an additional peak series at m/z 114, 126, 140, 148, 163, 198, and 213 (see arrows), apparently representing one or more components not found in the other batch. Attempts to help identify the unknown components by NMR and infrared failed because neither technique showed obvious differ-

ences between the two batches. Microscopic analysis, however, revealed that the batch with the unknown components contained a suspension or emulsion of small, basophilic particles.

Additional Py-HRMS, Py-TRMS, and Py-MS-MS studies have identified the unknown component as a quaternary (alkyl)ammonium compound, which was probably added to the polymer for the purpose of modifying its processing behavior.

This example demonstrates the value of Py-MS techniques for quality control of complex polymeric materials.

Quantitative analysis of polymer mixtures. A series of experiments on cross-linked, carbon-filled rubber triblend (provided by Dr. R. Lattimer, B. F. Goodrich) was carried out in order to investigate the feasibility of quantitative determination of polymer components by Py-MS (31). Multivariate statistical analysis of the data showed that the

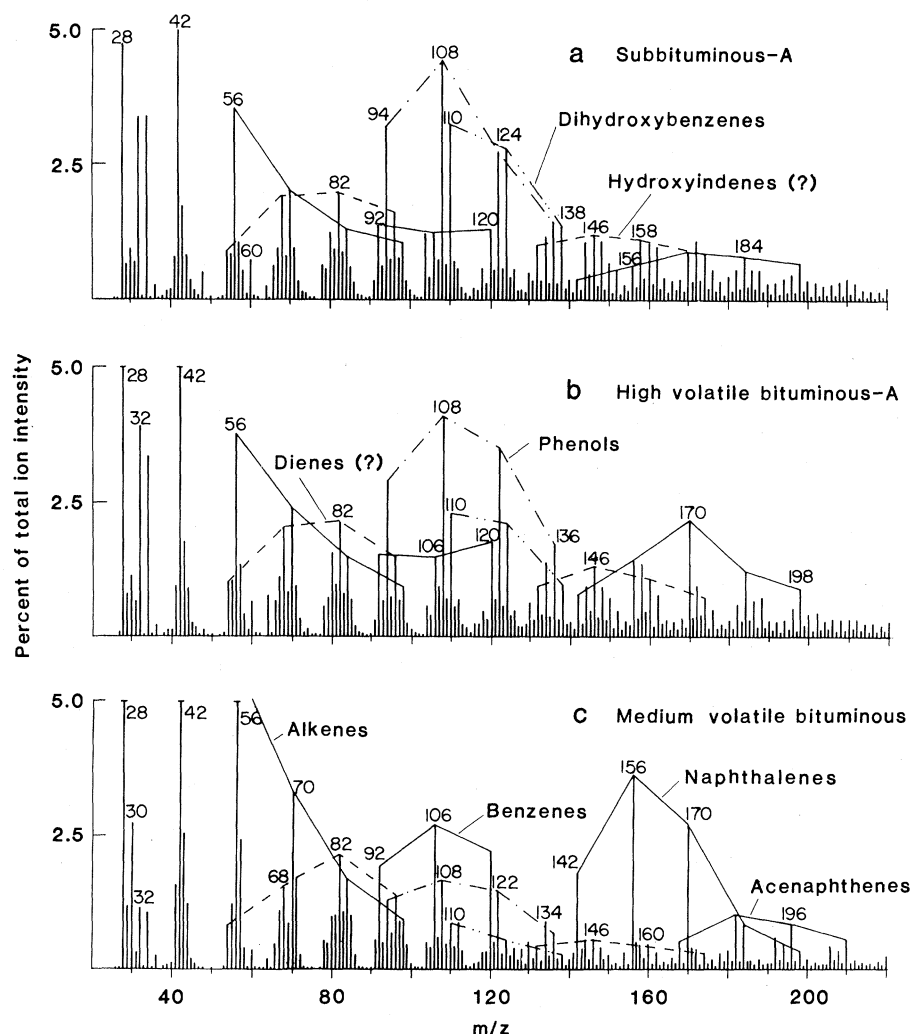


Fig. 5. Low-voltage Curie-point pyrolysis mass spectra of three coals of different rank representing the Uinta region of the Rocky Mountain coal province. Chemical labels are tentative and only represent the proposed dominant constituents of each peak series. For experimental conditions see legend to Fig. 3.

relative concentration of each of the three components could be directly determined from the Py-MS data with an average error in the 3 to 5 percent range. Although similar levels of precision are known to be obtainable by NMR and infrared, these techniques require much more elaborate and time-consuming sample preparation procedures for this type of relatively intractable polymeric material.

Further examples of quantitative analyses of polymer mixtures by Py-MS have been given by Windig *et al.* (24), who used a combination of factor analysis techniques and graphical rotation methods to analyze a ternary biopolymer mixture consisting of a protein (albumin), a polyhexose (glycogen), and an amino-sugar-containing polysaccharide (chondroitin sulfate). Again, it proved possible to determine the concentrations of the

individual components to within a few percent.

The most important conclusion which can be drawn from these quantitative studies is that, under the appropriate experimental conditions, pyrolysis processes in polymeric materials appear to be dominated by unimolecular decomposition reactions with little or no evidence of intermolecular (for example, recombination) reactions leading to the reformation of new or different pyrolyzates. Consequently, at first approximation the pyrolysis mass spectrum of a complex mixture of organic materials may be regarded as a linear combination of the spectra of the individual components. Nevertheless, matrix effects certainly play a role, especially with polar materials or in the presence of alkali cations (3), as can be inferred from careful factor analysis studies (7).

Numerical extraction of specific components from complex biological materials. Whereas the examples above involve relatively pure polymers and polymer mixtures, Py-MS techniques can be successfully applied to much more complex systems such as plant materials, coals, or microorganisms. A typical example of their application to complex biological samples (grass leaves) for the purpose of extracting specific component subpatterns correlated with a set of external measurements (susceptibility to insect attack) is given in Fig. 4. By using canonical variate analysis, a special factor analysis technique designed to find that linear combination of mass peak intensities (canonical variate function) best correlated with the relative intensity values of an external measurement for each sample, it proved possible to extract a relatively simple subpattern (Fig. 4b) from the complex Py-MS patterns of the grass leaves. As shown by comparison with the library spectrum (3) of natural rubber in Fig. 4c (obtained on a Curie-point Py-MS instrument in a different laboratory), the canonical variate pattern in Fig. 4b represents a typical poly-isoprenoid component in the grass leaves. The abundance of this poly-isoprenoid component shows a positive correlation (coefficient = 0.97) with the susceptibility of different grass species to attack by the grass bug *Labops hesperius*. Whether this points to a possible direct attraction of the insects to this particular substance or represents a more indirect relationship, needs further investigation (26).

Determination of key structural features in fossil organic matter. In spite of the complexity of grass leaves, the biochemical composition of such biological samples is relatively well defined. Coals and other fossil organic materials usually consist of heterogeneous mixtures of biological compounds which have undergone extensive degradation and chemical transformation over enormous time periods. What information can be obtained from Py-MS analysis of such extremely complex and ill-defined materials?

Results from a recent Py-MS study (32) on a set of over 100 coals from the Rocky Mountain Province are presented in Figs. 5 and 6. The spectra of three coals of different rank (degree of coalification) in Fig. 5 are found to be dominated by obvious series of homologous compounds such as alkenes, (alkyl)phenols, and (alkyl)naphthalenes. With increasing rank (from subbituminous to medium volatile bituminous) some component series (for instance, hydroxybenzenes) show a strong decrease whereas

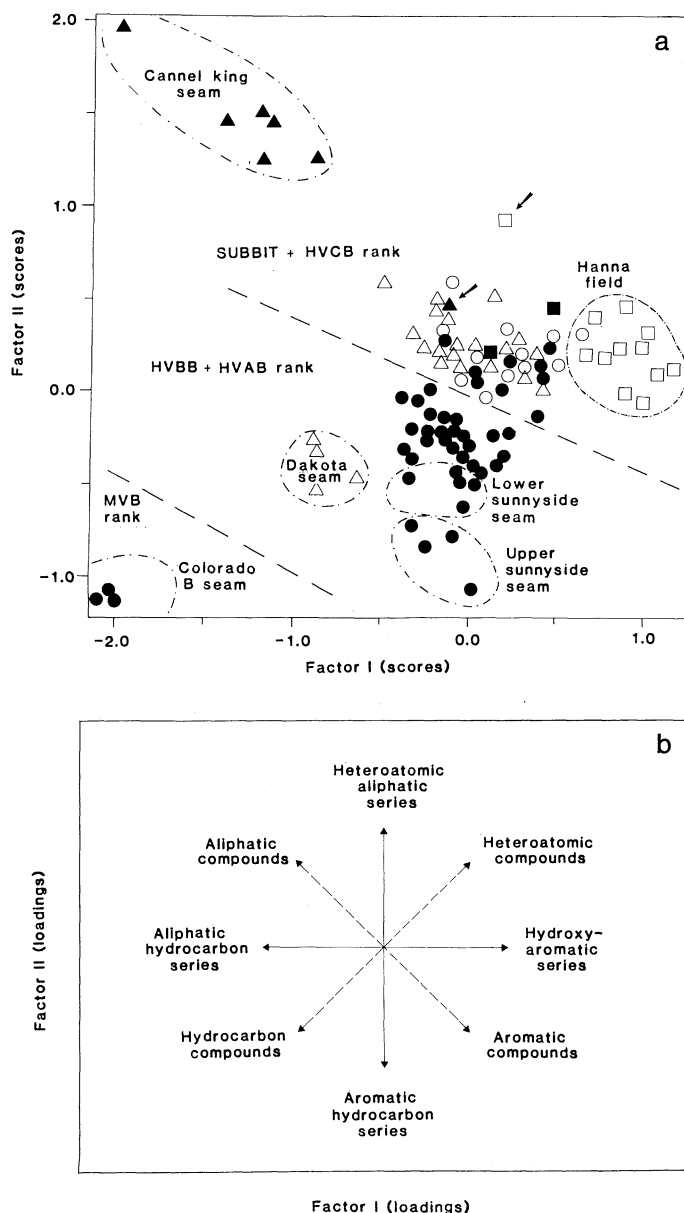


Fig. 6. (a) Score plot of the first two factors obtained from Curie-point pyrolysis mass spectra of over 100 coals from various regions (represented by different symbols) of the Rocky Mountain coal province. Note marked clustering of coals from different regions, fields, and seams (arrows point to outliers) as well as clear rank-related tendencies (indicated by dashed lines). (b) Highly schematized interpretation of the main underlying chemical tendencies in (a), obtained from the factor loading spectra in Fig. 7. Note the effects of a 45° rotation in the plane described by the two factors.

the relative abundance of other series (naphthalenes) increases markedly. The tendencies observed in Fig. 5 could be highlighted further by means of bivariate plots of selected mass peak intensities, for instance, m/z 110 versus m/z 156 (not shown). It should be pointed out, however, that tens of thousands of different bivariate plots could be composed with the several hundred peaks in a typical pyrolysis mass spectrum. Therefore, computerized multivariate analysis methods have become indispensable for evaluating and interpreting Py-MS data. In data sets with strongly correlated signals (the homologous ion series in Fig. 5) factor analysis methods provide an especially effective data reduction technique which often succeeds in explaining more than 90 percent of the total variance in the Py-MS data set with as few as five or six independent ("orthogonal") factors.

A plot of the first two factors for the Rocky Mountain coal data set, accounting for 36 percent of the total variance, is shown in Fig. 6a and reveals a distinct clustering of the various regions, fields, and seams in addition to a clear rank dependence. Each point in the plot represents a different coal sample obtained from the Pennsylvania State University Coal Sample Bank, where the samples were independently collected and stored for several years before being shipped to our laboratory for final sample preparation and Py-MS analysis. Therefore, the clustering tendencies in Fig. 6a indicate that the pyrolysis mass spectra obtained are truly representative of the different seams, fields, and regions and that the observed differences cannot be explained by sampling errors or instrumental bias. In conclusion, Py-MS proves to be a rapid and powerful classification method for coal samples of this type.

Perhaps even more important, however, is the information which can be obtained about the underlying chemical nature of the observed differences and tendencies in the data. Since both factors plotted in Fig. 6a are linear combinations of individual mass peak intensities, so-called factor loading spectra (23) can be constructed in which the relative contribution of each mass peak is visualized, as shown in Fig. 7. Careful inspection of Fig. 7 reveals that the interpretation of the factor loadings in broad chemical terms is relatively straightforward in this case. Apparently, the rank tendency in Fig. 6a corresponds to a chemical shift from aromatic heteroatom-containing compounds to aromatic hydrocarbons, whereas some of the more pronounced regional coal characteristics are due to different aromaticity/aliphaticity ratios.

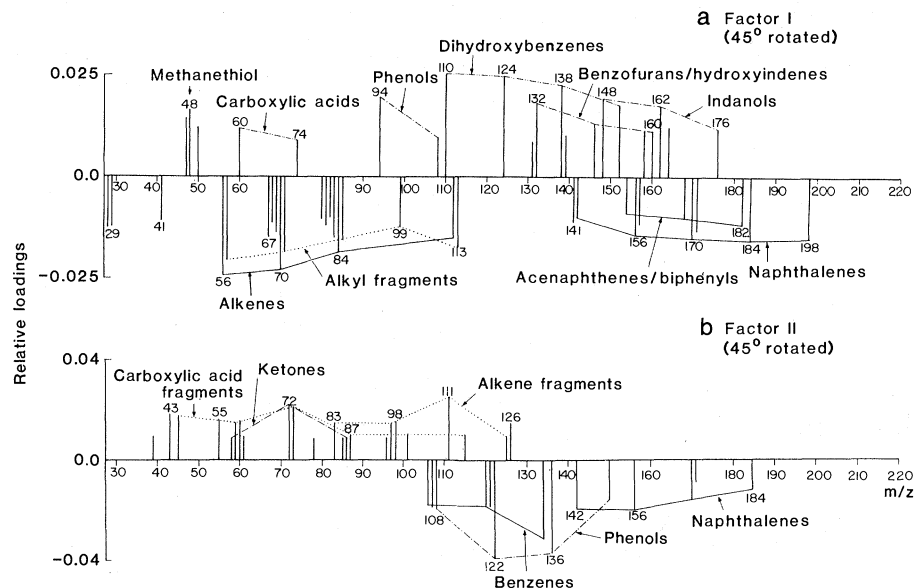


Fig. 7. Numerically extracted factor loadings (presented in the form of factor loading spectra) revealing major homologous ion series showing positive or negative correlations with both factors. Chemical labels are tentative. Note 45° rotation (visualized in Fig. 6b). The heteroatom-hydrocarbon separation in (a) may be thought to represent a typical rank (coalification) effect, whereas the aliphatic-aromatic separation in (b) appears to be due to differences in depositional environment (compare with Fig. 6a).

A highly schematic representation of the major chemical tendencies in the space spanned by the first two factors (and thus directly superimposable on the factor plot in Fig. 5b) is given in Fig. 6b. From these Py-MS results on coals it can be concluded that broad but highly useful chemical classes and key structural features can be established in spite of the extremely complex, heterogeneous nature of these materials.

Nonsupervised detection of chemical component axes. Although an encouraging degree of interlaboratory reproduc-

ibility has been demonstrated between groups using Curie-point Py-MS instruments of more or less standardized design (3, 12) [and notwithstanding the fact that hundreds of pyrolysis mass spectra obtained with these instruments are available from the literature, including an atlas with over 150 spectra of recent and fossil biomaterials (3)], chemical interpretation of pyrolysis mass spectra remains a difficult, often highly subjective enterprise. This is even more true when trying to interpret numerically extracted spectral patterns which may well

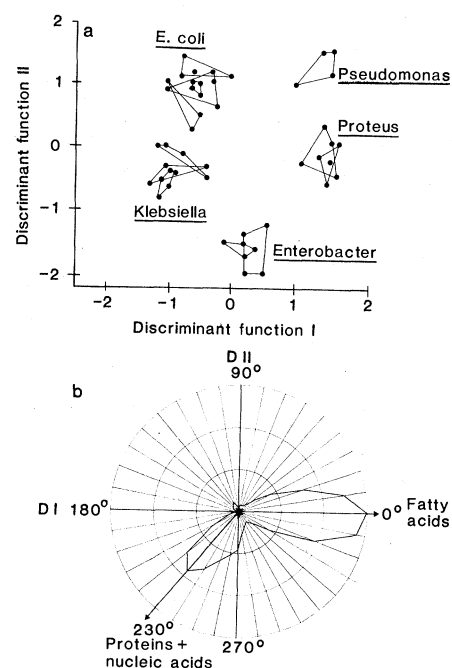


Fig. 8. (a) Score plot of the first two discriminant functions obtained from a set of 48 Curie-point pyrolysis mass spectra representing 12 bacterial strains isolated directly from human urine. Note successful separation of all five categories at the genus level. (b) Variance diagram displaying the total variance contribution of all mass variables found within consecutive 10° windows in the space described by the first two discriminant functions. Chemical interpretation of the two main component axes found at 0° and 230° was performed on the basis of the corresponding discriminant spectra (not shown).

represent components that cannot be separated by known physicochemical techniques (for instance, cross-linked polymer systems). Thus, exact reference spectra may be difficult or impossible to obtain. To further compound matters, mathematically extracted factors can be rotated in different directions (see Fig. 6b) with consequent changes in the corresponding chemical patterns. Therefore, it is important to develop nonsupervised techniques which can be used to find the optimal rotations ("axes") for the different chemical components in the data set by means of objective, mathematical criteria.

Recently, a first attempt at developing an automated approach to numerical extraction of unknown components from Py-MS data on complex organic materials was described by Windig and Meuzelaar (25). This approach, the so-called variance diagram technique, is demonstrated in Fig. 8, using Py-MS data on bacteria isolated directly from human urine and analyzed without prior culturing on nutrient media. By means of discriminant analysis, a special factor analysis method aimed at finding linear combinations of mass intensities with maximum discriminatory power for the various sample categories (discriminant functions), a promising degree of separation was obtained between bacterial isolates representing different genera belonging to the family of Enterobacteriaceae.

Obviously, the number of bacterial isolates in Fig. 8a is far too small for us to expect the calculated discrimination functions to remain stable when further bacterial isolates are added to the data set. However, as shown in Fig. 8b, the use of the variance diagram technique reveals two well-defined component axes in the space described by the first and second discriminant functions. Chemical interpretation of the "discriminant spectra" corresponding to the two component axes (at 0° and 230°C) in Fig. 8b revealed relatively simple patterns (not shown) with the axis at 0°C dominated by fatty acid signals and the axis at 230°C representing proteins and, to some extent, nucleic acids (33). Since possible chance associations between these

chemical components and the individual bacterial samples cannot be totally ruled out, this is by no means proof of the stability of the discriminant solution shown in Fig. 8a. Nevertheless, the observation of well-defined chemical tendencies practically eliminates the possibility of a chance separation due to random fluctuations in the data set.

The latter danger is especially imminent in small data sets where the number of samples is lower than the number of independent variables. At first sight, this problem may appear to be difficult to avoid when using pyrolysis mass spectra containing hundreds of mass peaks. As mentioned before, however, the high degree of redundancy in the spectra caused by the presence of strongly correlating peak series usually reduces the "intrinsic dimensionality" to only five or six orthogonal factors. Therefore, we routinely perform discriminant analysis on the dozen or so most significant factors only (23).

As demonstrated in Fig. 8, the variance diagram technique can be very helpful in locating the major chemical component axes. Moreover, preliminary tests have indicated the feasibility of using library search techniques to obtain "best matches" between component spectra extracted by the variance diagram method and reference spectra representing different classes of biochemical compounds. Further development of automated methods along these lines should greatly facilitate the task of evaluating and interpreting pyrolysis mass spectra of complex organic materials, thus making the technique more accessible to the nonspecialist.

References and Notes

1. M. Barber *et al.*, *Biomed. Mass Spectrom.* **11**, 182 (1984).
2. W. J. Irwin, *Analytical Pyrolysis—A Comprehensive Guide* (Dekker, New York, 1982), chapters 2, 4, and 5.
3. H. L. C. Meuzelaar, J. Haverkamp, F. D. Hileman, *Pyrolysis Mass Spectrometry of Recent and Fossil Biomaterials—Compendium and Atlas* (Elsevier, Amsterdam, 1982), chapters 1 to 7.
4. P. D. Zeman, *Anal. Chem.* **24**, 1709 (1952).
5. H.-R. Schulten and R. P. Lattimer, *Mass Spectrom. Rev.* **3**, 231 (1984).
6. Extranuclear Labs. Inc., Pittsburgh, Pa. (model 5000-1 quadrupole Curie-point Py-MS system), V.G. Gas Analysis Ltd., Middlewich, United Kingdom, and Stamford, Conn. (magnetic Curie-point Py-MS system).
7. W. Windig, P. G. Kistemaker, J. Haverkamp, H. L. C. Meuzelaar, *J. Anal. Appl. Pyrol.* **2**, 7 (1980).
8. Ch. Bühler, thesis, ETH Zürich, Switzerland (1971), pp. 70–73.
9. H. Giacobbo and W. Simon, *Pharm. Acta Helv.* **39**, 162 (1964).
10. H. L. C. Meuzelaar and P. G. Kistemaker, *Anal. Chem.* **45**, 587 (1973).
11. H. L. C. Meuzelaar and S. M. Huff, *J. Anal. Appl. Pyrol.* **3**, 111 (1981).
12. Laboratories with more or less compatible, dedicated Curie-point Py-MS systems: Colorado School of Mines (K. J. Voorhees); University of Utah (H. L. C. Meuzelaar); Ministry of Health, Toronto (R. Kajioka); Cadbury Schweppes, London (C. S. Gutteridge); Institute for Medical Genetics, Moscow (A. Antoschekkin); and FOM Institute for Atomic and Molecular Physics, Amsterdam (J. J. Boon).
13. H. L. C. Meuzelaar, M. A. Posthumus, P. G. Kistemaker, *J. Kistemaker, Anal. Chem.* **45**, 1546 (1973).
14. P. G. Kistemaker, A. J. H. Boerboom, H. L. C. Meuzelaar, in *Dynamic Mass Spectrometry*, D. Price and J. F. J. Todd, Eds. (Heyden, London, 1975), vol. 4, pp. 139–152.
15. H.-R. Schulten and W. Görtz, *Anal. Chem.* **50**, 428 (1978).
16. H.-R. Schulten and U. Bahr, *J. Anal. Appl. Pyrol.* **5**, 27 (1983).
17. H.-R. Schulten, H. D. Beckey, A. J. H. Boerboom, H. L. C. Meuzelaar, *Anal. Chem.* **45**, 2358 (1973).
18. T. H. Risby and A. L. Yergey, *ibid.* **50**, 327A (1978).
19. A. M. Harper, H. L. C. Meuzelaar, G. S. Metcalf, D. L. Pope, in *Analytical Pyrolysis—Techniques and Applications*, K. J. Voorhees, Ed. (Butterworth, London, 1984), pp. 157–195.
20. W. Eshuis, H. L. C. Meuzelaar, D. L. Pope, unpublished software (NORMA program suitable for HP 21MX computer system available through H.L.C.M.).
21. B. R. Kowalski, *Anal. Chem.* **47**, 1152A (1975); ARTHUR program available from Infometrix, P.O. Box 25888, Seattle, Wash. 98125.
22. *Statistical Package for the Social Sciences (SPSS)*, N. H. Nie *et al.*, Eds. (McGraw-Hill, New York, ed. 2, 1975).
23. W. Windig, P. G. Kistemaker, J. Haverkamp, *J. Anal. Appl. Pyrol.* **3**, 199 (1981).
24. W. Windig, J. Haverkamp, P. G. Kistemaker, *Anal. Chem.* **55**, 81 (1983).
25. W. Windig and H. L. C. Meuzelaar, *ibid.*, in press.
26. _____, B. A. Haws, W. F. Campbell, K. H. Asay, *J. Anal. Appl. Pyrol.* **5**, 183 (1983).
27. W. Eshuis, P. G. Kistemaker, H. L. C. Meuzelaar, in *Analytical Pyrolysis*, C. E. R. Jones and C. A. Cramers, Eds. (Elsevier, Amsterdam, 1977), pp. 151–166.
28. S. Wold and M. Sjöström, in *Chemometrics: Theory and Application*, B. R. Kowalski, Ed. (ACS Symposium Series 52, American Chemical Society, Washington, D.C., 1977), pp. 243–282.
29. H.-J. Düssel, N. Wenzel, D. O. Hummel, *Angew. Makromol. Chem.* **106**, 107 (1982).
30. J. M. Richards *et al.*, *Macromolecules*, in press.
31. R. P. Lattimer, paper presented at the 6th International Symposium on Analytical and Applied Pyrolysis, Wiesbaden, Federal Republic of Germany, September 1984.
32. H. L. C. Meuzelaar, A. M. Harper, G. R. Hill, P. H. Given, *Fuel* **63**, 640 (1984).
33. H. L. C. Meuzelaar, paper presented at the 5th International Symposium on Mass Spectrometry in Life Sciences, Ghent, Belgium, May 1984.
34. The generous help and advice of G. R. Hill, P. Given, and W. J. Kolff throughout various stages of the work described here is gratefully acknowledged. The research reported in this article was supported by funds from the Department of Energy (contract DE-FG 82-PC50970), the Army Research Office (contract DAAG29-84-K-0009), and the state of Utah.